J. Fluid Mech. (1995), *vol.* 287, *pp.* 133–150

The stability of an interface between viscous fluids subjected to a high-frequency magnetic field and consequences for electromagnetic casting

By DEEPAK† AND J. W. EVANS‡

Department of Materials Science and Mineral Engineering, University of California, Berkeley CA 94720, USA

(Received 4 October 1993 and in revised form 26 October 1994)

The stability of an interface between inviscid fluids subjected to a high-frequency magnetic field has been examined previously by Garnier & Moreau (1983). The present paper extends that study to include the viscosity of both fluids in order to estimate the damping rates of the perturbations. Furthermore, Garnier & Moreau made an assumption that the frequency of oscillation of the interface could be neglected compared to the frequency of the applied field; they concluded that the applied field was not destabilizing. That (apparently reasonable) assumption has been lifted in the present work and the consequence is that the magnetic field is seen to lead to instability over a significant range of wavelengths. Application of this analysis to the electromagnetic casting of aluminium is discussed.

1. Introduction

Electromagnetic casting of aluminium is a continuous operation without the mould which is used in the conventional method of casting. An alternating current passing through an inductor around the liquid metal produces a magnetic field in it. Consequently the current induced in the metal, together with this magnetic field, generate a force to support the metal from the sides. The weight of the melt is supported on the metal that has already solidified.

Sometimes, after electromagnetic casting of aluminium, horizontal striations are observed on the surface of the cast ingot. These striations may be caused by the wave-like motion of the free liquid surface that travels to the point of solidification on the surface during the casting operation. The oscillatory motion at the liquid free surface is a result of the perturbations (disturbances) that may be generated by an external source such as vibrations in the bottom block supporting the ingot. It is further noted that the striations on the surface of the cast ingot are not reproducible, which in turn supports the possibility that the perturbation of the liquid surface causes the striations because these perturbations are also random in nature.

The striations present on the surface have a deleterious effect during the subsequent steps in production of metal sheets from the ingot. For example, in the rolling operation to manufacture thin metal sheets, the striations produce defects that cause failure in the materials. Hence it may become necessary to either discard the ingot or first machine a few centimetres of metal off the ingot to generate a flat surface. With

† Present address: Motorola Inc., 5005 E. McDowell Road, D-304, Phoenix AZ 85008, USA.
‡ To whom correspondence should be addressed.

this practical consequence in mind, here we examine the possibility of oscillations on the surface that may produce striations. Stated alternatively, it will not be possible to attribute these striations to a random perturbation if it is damped faster than the time taken for a disturbance to travel to the solidification point on the surface.

In the context of stability analysis of fluids, several hydrodynamic instabilities arise, notably Rayleigh–Taylor and Kelvin–Helmholtz instabilities. In both of these cases, a small perturbation of a fluid interface causes it to deform further. Chandrasekhar (1981) has shown that in the presence of a steady (time-independent) magnetic field, the hydrodynamic systems above generally become more stable.

Many more linear stability analyses, based on normal mode expansions of the perturbed quantities, have been applied to systems in aluminium processing. The ones with a steady magnetic field are encountered in aluminium reduction cells (Sneyd 1992; Rivat, Etay & Garnier 1991; Zimin & Kolpakov 1990). Sneyd (1992) showed that the magnetic field is mostly stabilizing, except at large wavelengths in a system where the interface is crossed by an intense current. Rivat *et al.* (1991) have determined that a vertical magnetic field always has a stabilizing effect on the gravity waves in an electrically conducting medium present in an aluminium reduction cell.

Another application of stability analysis is in horizontal electromagnetic (EM) casting, where both the steady magnetic field and current may be used to support the weight of the liquid metal. Takeuchi, Etay & Garnier (1989) have conducted such an analysis on the free surfaces encountered in horizontal casting of steep strips and rods.

The issue of stability in the levitation of a thin metal sheet by a high-frequency (kHz) magnetic field was studied both experimentally and analytically by Hull, Wiencek & Rote (1989). There the instability is primarily of Rayleigh–Taylor type in the presence of EM fields. A review of various stability analyses in EM processing area has been done by Fautrelle (1991). His coworkers, Galpin *et al.* (1990), have also experimentally investigated the effect of an alternating magnetic field on liquid metals in the low-frequency range. In that study, unlike the present work, the fluid motion is influenced not only by the mean part of the EM force but also by the alternating part.

The focus of the present work is on vertical EM casting of aluminium supported by a high-frequency magnetic field. At such frequencies, the skin depth for the fields in the metal is small. Because the metal is not substantially penetrated by the magnetic field, the field is essentially parallel to the surface of the metal. Furthermore, because the magnetic field diffuses into the metal to a millimetre or so, and the cross-section and depth of liquid metal pool are on the order of 1 m^2 and a few centimetres, respectively, the extent of the liquid metal both in the horizontal direction and in the depth can be considered infinite.

Under these circumstances, the work by McHale & Melcher (1982), and Garnier & Moreau (1983) applies in determining the stability of the EM casting operation. Although McHale & Melcher's analysis considers both a viscous fluid and the interfacial perturbation, their attention is on the instability that arises in the bulk of the fluid. In fact, in the first set of their results, a flat interface is bounded by rigid insulating material. Later, the effect of interfacial perturbation, which is the main concern of the present work, is simply added on and a conclusion is drawn that it does not significantly alter the results obtained with a flat interface. Thus, the instability considered there is purely due to bulk coupled mechanisms. Winstead & Hoburg (1991) have extended that study to include the electrothermal effects on the incipience of the instability.

Garnier & Moreau's (1983) work, on the other hand, deals purely with the disturbance on the liquid metal surface. They consider inviscid fluids and, in terms of

stability analysis, a system similar to that for EM casting of aluminium is always stable. However, the marginal state is determined to be oscillatory. That is, any imposed perturbations on the liquid metal surface will neither grow nor damp. Because the surface executes an undamped oscillation, from a practical point of view, this situation could clearly allow formation of striations on the cast metal ingot.

The viscosity (neglected in Garnier & Moreau's work) is likely to damp these oscillations of the surface. Therefore, in the present work we have extended their analysis by including the viscous effects in order to estimate the damping rates. A low damping rate, for all practical purposes, would still permit the possibility of striations on the ingot.

Also, in that analysis Garnier & Moreau ignored the frequency of the normal modes of the disturbance (s) in comparison to the applied frequency of the magnetic field (ω). Although s may be much smaller than ω, there is no need to ignore s in writing the perturbed magnetic field. We have avoided that approximation and the results are shown to substantially change their conclusions.

2. Linear stability analysis

Two viscous fluids, identified by subscripts 1 and 2, are separated by an interface $z = \Phi(\boldsymbol{r}, t)$, as shown in figure 1, where in general, the vertical location of the interface at any position and time is determined by specifying the position vector, $\boldsymbol{r} = i\hat{x} + y\hat{y}$.

The initial equilibrium state of the system is defined by a flat interface, $z = 0$, and the fluids are at rest. In general, with the fluid in motion, the magnetic field follows the equation

$$\frac{1}{\mu_0 \sigma} \nabla^2 \boldsymbol{B} + \nabla \times (\boldsymbol{V} \times \boldsymbol{B}) = \frac{\partial \boldsymbol{B}}{\partial t},$$

where μ_0 is the permeability of free space, σ the electrical conductivity of fluid 1, $\boldsymbol{B}$ the magnetic flux density and $\boldsymbol{V}$ the fluid velocity. In many applications, such as electromagnetic casting of aluminium, the metal conductivity is large and the fluid velocities are small; thus the magnetic Reynolds number (based on skin depth δ and the y-component of the perturbed fluid velocity v or angular frequency of applied magnetic field ω)

$$R_m = \sigma \mu_0 v \delta = \left(\frac{2\mu_0 \sigma}{\omega}\right)^{1/2} v$$

is small. For example, for values typical in electromagnetic casting of aluminium, $\sigma = 3.85 \times 10^6$ mho m^{-1}, $\omega = 2\pi \times 10^3$ rad s^{-1} and $v = 0.10$ m s^{-1}, $R_m (= 0.004) \ll 1$. In that case the convective term in the equation above can be neglected and a uniform flux density of angular frequency ω, applied in the fluid 2, diffuses into the fluid 1 according to the equation and the constraint (Garnier & Moreau 1983), respectively:

$$\frac{1}{\mu_0 \sigma} \nabla^2 \boldsymbol{B}_1 = \frac{\partial \boldsymbol{B}_1}{\partial t}, \tag{1}$$

$$\nabla \cdot \boldsymbol{B}_1 = 0. \tag{2}$$

Using the superscript 0 to denote the initial state, the applied magnetic flux density,

$$\boldsymbol{B}_2^0(z, t) = B_0 \cos(\omega t)\, \hat{x}, \quad z > 0 \tag{3}$$

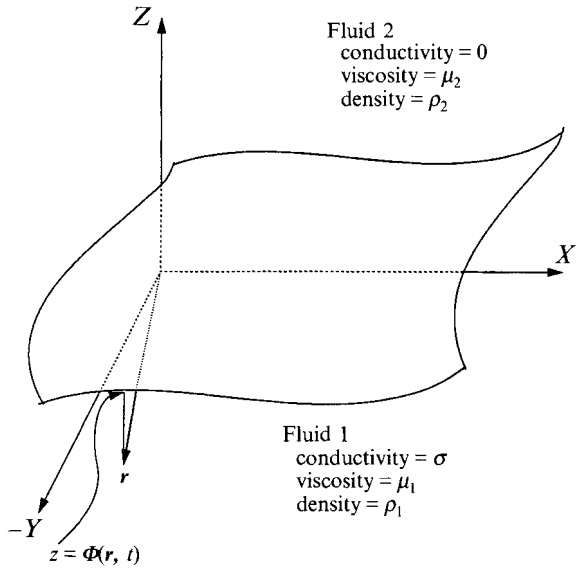

FIGURE 1. Coordinate system and relative location of fluids.

satisfies the following equation and two constraints, respectively:

$$\nabla^2 \boldsymbol{B}_2 = 0, \tag{4}$$

$$\nabla \cdot \boldsymbol{B}_2 = 0, \tag{5}$$

$$\nabla \times \boldsymbol{B}_2 = 0, \tag{6}$$

and then the solution of the field in $z < 0$ from (1) is

$$\boldsymbol{B}_1^0(z, t) = B_0 \, \mathrm{e}^{z/\delta} \cos(\omega t + z/\delta)\, \hat{\boldsymbol{x}}, \quad z < 0, \tag{7}$$

where $\delta = (2/\mu_0 \sigma \omega)^{1/2}$ is the skin depth of penetration of the field in the conducting fluid.

The motion of the fluid is described by the continuity and Navier–Stokes equations. In addition to gravity, the conducting fluid 1 also experiences an electromagnetic (EM) body force $\boldsymbol{J}_1 \times \boldsymbol{B}_1$, where, from Ampere's law, current density $\boldsymbol{J}_1 = (1/\mu_0) \nabla \times \boldsymbol{B}_1$. Therefore, for fluid 1,

$$\nabla \cdot \boldsymbol{V}_1 = 0, \tag{8}$$

$$\rho_1 \left[\frac{\partial \boldsymbol{V}_1}{\partial t} + (\boldsymbol{V}_1 \cdot \nabla)\, \boldsymbol{V}_1 \right] = -\nabla P_1 + \mu_1 \nabla^2 \boldsymbol{V}_1 + \boldsymbol{J}_1 \times \boldsymbol{B}_1 - \rho_1 g \hat{\boldsymbol{z}}, \tag{9}$$

where ρ denotes density, P pressure and g gravity, and similarly for fluid 2 with $\boldsymbol{J} \times \boldsymbol{B}$ set to zero.

In the case of inviscid fluids, such as those considered by Garnier & Moreau (1983), the fluid velocities in the initial equilibrium state are arbitrary in the horizontal direction. Because of the requirement of continuity of the velocities at the interface for viscous fluids, the velocities are not arbitrary. In the initial state employed here the fluids are at rest. Thus, we omit the possibility of Kelvin–Helmholtz instability in the present analysis.

Garnier & Moreau (1983) have shown that fluid 1 experiences only the mean part

(time averaged) of the EM forces, for the inertia of the fluid does not permit it to oscillate at a high frequency (kHz) of 2ω. Thus, the time-averaged force,

$$\langle \boldsymbol{J}_1^0 \times \boldsymbol{B}_1^0 \rangle = -\frac{B_0^2}{2\mu_0 \delta} e^{2z/\delta} \hat{z},$$

is substituted in (8) and then the pressure in the initial state is determined to be

$$P_1^0(z) = P_0 - \rho_1 g z + \frac{B_0^2}{4\mu_0}(1 - e^{2z/\delta}), \tag{10}$$

$$P_2^0(z) = P_0 - \rho_2 g z \tag{11}$$

for $P_1^0 = P_2^0 = P_0$ at $z = 0$.

Now a disturbance is imposed on the interface in its initial equilibrium state. This disturbance is expanded in its normal modes, and then the stability of the system is examined with respect to each of those modes. An arbitrary normal mode of the imposed perturbation is written as $\eta = \epsilon_0 e^{i(st + \boldsymbol{k}\cdot\boldsymbol{r})}$, where the real vector $\boldsymbol{k} = [k_x, k_y, 0]$ and s is complex.

2.1. *Perturbation of the electromagnetic fields*

The perturbation of the magnetic field yields in general

$$\frac{1}{\sigma\mu_0}\nabla^2 \boldsymbol{b} + \nabla \times (\boldsymbol{v} \times \boldsymbol{B}) + \nabla \times (\boldsymbol{V} \times \boldsymbol{b}) = \frac{\partial \boldsymbol{b}}{\partial t}.$$

A detailed order-of-magnitude analysis performed by Garnier & Moreau (1983, p. 371) demonstrates that the convective terms can again be neglected. Therefore, the linearized equations that govern the perturbed fields are directly obtained from (1) and (4):

$$\nabla^2 \boldsymbol{b}_2 = 0, \tag{12}$$

$$\frac{1}{\mu_0 \sigma}\nabla^2 \boldsymbol{b}_1 = \frac{\partial \boldsymbol{b}_1}{\partial t}. \tag{13}$$

According to the constraints in (2), (5) and (6), up to linear terms the perturbed field both in $z > 0$ and $z < 0$ are solenoidal, and also the field in $z > 0$ is curl free.

At $z = 0$, from continuity of the magnetic field (Garnier & Moreau 1983),

$$b_{1y} = b_{2y}, \quad b_{1z} = b_{2z}, \quad b_{1x} - b_{2x} = -i\frac{B_0 \epsilon_0}{\sqrt{2\delta}}(e^{i\theta_1} - e^{i\theta_2}). \tag{14a–c}$$

where $\theta_1 = (s+\omega)t + \boldsymbol{k}\cdot\boldsymbol{r} - \pi/4$, $\theta_2 = (s-\omega)t + \boldsymbol{k}\cdot\boldsymbol{r} + \pi/4$, and ϵ_0 is the amplitude of the interface perturbation.

The boundary condition (14*c*) suggests that the solution of the perturbed magnetic flux density has form $\boldsymbol{b} = \boldsymbol{f}(z) e^{i\theta_1} + \boldsymbol{g}(z) e^{i\theta_2}$ (Garnier & Moreau 1983). After substituting each term of the preceding equation in (12) and (13) and realizing that the perturbed fields $\boldsymbol{b}_1$ at $z = -\infty$ and $\boldsymbol{b}_2$ at $z = \pm\infty$ diminish to a zero value, up to four vector constants, $\boldsymbol{E}$, $\boldsymbol{F}$, $\boldsymbol{G}$ and $\boldsymbol{H}$, the magnetic flux density is determined to be

$$\boldsymbol{b}_1 = \boldsymbol{E} e^{i\theta_1 + \gamma_+ z} + \boldsymbol{F} e^{i\theta_2 + \gamma_- z},$$

$$\boldsymbol{b}_2 = \boldsymbol{G} e^{i\theta_1 - kz} + \boldsymbol{H} e^{i\theta_2 - kz},$$

where†

$$\gamma_+^2 = k^2 + i\mu_0\sigma(s+\omega), \quad \gamma_-^2 = k^2 + i\mu_0\sigma(s-\omega). \tag{15a, b}$$

† In the following equations, Garnier & Moreau (1983) neglected s in comparison to ω. That approximation is avoided here, and later shown to have a significant effect.

Then with the help of the boundary conditions in (14) and the constraints, the perturbed magnetic flux density is completely established:

$$b_{1x} = -\mathrm{i}\frac{B_0\epsilon_0}{\sqrt{2\delta}}\left[\frac{k_y^2+\gamma_+ k}{k(\gamma_+ +k)}\,\mathrm{e}^{\mathrm{i}\theta_1+\gamma_+ z} - \frac{k_y^2+\gamma_- k}{k(\gamma_- +k)}\mathrm{e}^{\mathrm{i}\theta_2+\gamma_- z}\right], \tag{16a}$$

$$b_{1y} = \mathrm{i}\frac{B_0\epsilon_0}{\sqrt{2\delta}}\left[\frac{k_x k_y}{k(\gamma_+ +k)}\,\mathrm{e}^{\mathrm{i}\theta_1+\gamma_+ z} - \frac{k_x k_y}{k(\gamma_- +k)}\mathrm{e}^{\mathrm{i}\theta_2+\gamma_- z}\right], \tag{16b}$$

$$b_{1z} = -\frac{B_0\epsilon_0}{\sqrt{2\delta}}\left[\frac{k_x}{(\gamma_+ +k)}\,\mathrm{e}^{\mathrm{i}\theta_1+\gamma_+ z} - \frac{k_x}{(\gamma_- +k)}\mathrm{e}^{\mathrm{i}\theta_2+\gamma_- z}\right], \tag{16c}$$

$$b_{2x} = \mathrm{i}\frac{B_0\epsilon_0}{\sqrt{2\delta}}\left[\frac{k_x^2}{k(\gamma_+ +k)}\,\mathrm{e}^{\mathrm{i}\theta_1-kz} - \frac{k_x^2}{k(\gamma_- +k)}\mathrm{e}^{\mathrm{i}\theta_2-kz}\right], \tag{16d}$$

$$b_{2y} = \mathrm{i}\frac{B_0\epsilon_0}{\sqrt{2\delta}}\left[\frac{k_x k_y}{k(\gamma_+ +k)}\,\mathrm{e}^{\mathrm{i}\theta_1-kz} - \frac{k_x k_y}{k(\gamma_- +k)}\mathrm{e}^{\mathrm{i}\theta_2-kz}\right], \tag{16e}$$

$$b_{2z} = -\frac{B_0\epsilon_0}{\sqrt{2\delta}}\left[\frac{k_x}{(\gamma_+ +k)}\,\mathrm{e}^{\mathrm{i}\theta_1-kz} - \frac{k_x}{(\gamma_- +k)}\mathrm{e}^{\mathrm{i}\theta_2-kz}\right]. \tag{16f}$$

2.2. *Perturbation of the fluid motion*

The equation of motion that describes the perturbation velocities is obtained after linearization of (8) and (9),

$$\nabla\cdot\boldsymbol{v}_1 = 0, \tag{17a}$$

and after using the fact that neither the density nor the viscosity of the fluids is perturbed for an incompressible fluid,

$$\rho_1\frac{\partial\boldsymbol{v}_1}{\partial t} = -\nabla p_1 + \mu_1\nabla^2\boldsymbol{v}_1 + \boldsymbol{J}_1^0\times\boldsymbol{b}_1 + \boldsymbol{j}_1\times\boldsymbol{B}_1^0, \quad z<0. \tag{17b}$$

Similarly, for the non-conducting fluid,

$$\nabla\cdot\boldsymbol{v}_2 = 0, \tag{18a}$$

$$\rho_2\frac{\partial\boldsymbol{v}_2}{\partial t} = -\nabla p_2 + \mu_2\nabla^2\boldsymbol{v}_2, \quad z>0. \tag{18b}$$

The current induced due to the disturbance of the interface is obtained by considering the first-order terms in Ampere's law. That is, $\boldsymbol{j}_1 = (1/\mu_0)\nabla\times\boldsymbol{b}_1$. Thus, the components of the current density, $\boldsymbol{j}_1$, are

$$j_{1x} = -\mathrm{i}\frac{B_0\epsilon_0}{\sqrt{2\delta\mu_0}}\left[\frac{k_x k_y}{(\gamma_+ +k)}\left(1+\frac{\gamma_+}{k}\right)\mathrm{e}^{\mathrm{i}\theta_1+\gamma_+ z} - \frac{k_x k_y}{(\gamma_- +k)}\left(1+\frac{\gamma_-}{k}\right)\mathrm{e}^{\mathrm{i}\theta_2+\gamma_- z}\right], \tag{19a}$$

$$j_{1y} = -\mathrm{i}\frac{B_0\epsilon_0}{\sqrt{2\delta\mu_0}}\left[\frac{\gamma_+ k-k_x^2}{k}\,\mathrm{e}^{\mathrm{i}\theta_1+\gamma_+ z} - \frac{\gamma_- k-k_x^2}{k}\,\mathrm{e}^{\mathrm{i}\theta_2+\gamma_- z}\right], \tag{19b}$$

$$j_{1z} = -\frac{B_0\epsilon_0}{\sqrt{2\delta\mu_0}}[k_y\,\mathrm{e}^{\mathrm{i}\theta_1+\gamma_+ z} - k_y\,\mathrm{e}^{\mathrm{i}\theta_2+\gamma_- z}]. \tag{19c}$$

Again, because the fluid experiences only the electromagnetic body forces that are time averaged over the oscillating frequency of 2ω above and below the interface perturbation frequency s, the force considered in (17) is $\langle \boldsymbol{J}_1^0\times\boldsymbol{b}_1 + \boldsymbol{j}_1\times\boldsymbol{B}_1^0\rangle$. This

averaged force may be written as $\eta \boldsymbol{f}$, because the normal modes of the body forces are also proportional to the perturbation of the interface. Hence, after time averaging, the components of $\boldsymbol{f}$ are

$$f_x = \mathrm{i}\frac{B_0^2 k_x}{2\mu_0 \delta^2}\left[\frac{1}{(\gamma_+ + k)}\mathrm{e}^{\alpha_+ z} + \frac{1}{(\gamma_- + k)}\mathrm{e}^{\alpha_- z}\right], \tag{20a}$$

$$f_y = -\frac{B_0^2 k_y}{4\mu_0 \delta}[(1-\mathrm{i})\,\mathrm{e}^{\alpha_+ z} - (1+\mathrm{i})\,\mathrm{e}^{\alpha_- z}], \tag{20b}$$

$$f_z = \frac{B_0^2}{2\mu_0 \delta^2}\left[\left(\frac{k_y^2 + \gamma_+ k}{k(\gamma_+ + k)} - \frac{1+\mathrm{i}}{2}\frac{\delta}{k}(k_x^2 - \gamma_+ k)\right)\mathrm{e}^{\alpha_+ z} + \left(\frac{k_y^2 + \gamma_- k}{k(\gamma_- + k)} - \frac{1-\mathrm{i}}{2}\frac{\delta}{k}(k_x^2 - \gamma_- k)\right)\mathrm{e}^{\alpha_- z}\right], \tag{20c}$$

where $\alpha_+ = \gamma_+ + (1-\mathrm{i})/\delta$ and $\alpha_- = \gamma_- + (1+\mathrm{i})/\delta$.

From (17) and (20), it is clear that the normal modes for the perturbed velocities are similar to those for the perturbed interface. Thus, in both the fluids, $\boldsymbol{v} = [u, v, w] \sim \mathrm{e}^{\mathrm{i}(st + \boldsymbol{k}\cdot\boldsymbol{r})}$. Using this normal mode expansion in (17), with $\mathrm{D} \equiv \partial/\partial z$, in $z < 0$, the linearized continuity condition is written as

$$\mathrm{i}k_x u_1 + \mathrm{i}k_y v_1 + \mathrm{D}w_1 = 0, \tag{21}$$

while combining the x- and y-components of the perturbation velocity with (21) gives the perturbation pressure:

$$\mathrm{i}k^2 p_1 = s\rho_1 \mathrm{D}w_1 + \mathrm{i}\mu_1(\mathrm{D}^2 - k^2)\mathrm{D}w_1 + \eta(\boldsymbol{k}\cdot\boldsymbol{f}). \tag{22}$$

Further, using this equation to eliminate p_1 from the z-component of velocity yields

$$(\mathrm{D}^2 - k^2)[\rho_1 s + \mathrm{i}\mu_1(\mathrm{D}^2 - k^2)]\,w_1 = \eta[\mathrm{i}k^2 f_z - \mathrm{D}(\boldsymbol{k}\cdot\boldsymbol{f})]. \tag{23}$$

Similarly for fluid 2 in $z > 0$, from (18) the relevant equations of motion are

$$\mathrm{i}k^2 p_2 = s\rho_2 \mathrm{D}w_2 + \mathrm{i}\mu_2(\mathrm{D}^2 - k^2)\mathrm{D}w_2, \tag{24}$$

$$(\mathrm{D}^2 - k^2)[\rho_2 s + \mathrm{i}\mu_2(\mathrm{D}^2 - k^2)]\,w_2 = 0. \tag{25}$$

In the following, with the boundary conditions on w specified below, (23) and (25) are used to determine the fluid velocities, which in turn are used to obtain the perturbation pressures at the interface from (22) and (24). Finally, from the condition of discontinuity in pressure across a curved interface, a stability criterion is established.

The perturbed velocities in both the fluids diminish away from the interface. Therefore,

$$w_1 = 0, \quad z = -\infty, \tag{26a}$$

$$w_2 = 0 \quad z = +\infty. \tag{26b}$$

Furthermore, the kinematic boundary condition at the interface demands that a fluid particle at the interface remains there during the perturbation. Mathematically,

$$\mathrm{i}s\eta = w_1 = w_2, \quad z = 0. \tag{27}$$

Also, up to linear terms, the tangential velocities u and v are continuous at the interface. Therefore, because the flow is solenoidal, from an equation of type (21), it can be deduced that $\mathrm{D}w$ is also continuous. That is,

$$\mathrm{D}w_1 = \mathrm{D}w_2, \quad z = 0. \tag{28}$$

The dynamic boundary condition can be written by realizing that the normal component of the stress experiences a discontinuity across a curved interface, while the

tangential component is continuous. The latter requirement up to first order is expressed as

$$\mu_1(\mathrm{D}^2+k^2)\,w_1 = \mu_2(\mathrm{D}^2+k^2)\,w_2, \quad z=0. \tag{29}$$

The discontinuity in the normal component of the stress across an interface defined by $z=\Phi$ is (Gupta 1993)

$$P_2-P_1+2\mu_1\,\hat{\boldsymbol{n}}\cdot[(\hat{\boldsymbol{n}}\cdot\nabla_1)\,V_1]-2\mu_2\,\hat{\boldsymbol{n}}\cdot[(\hat{\boldsymbol{n}}\cdot\nabla)\,V_2]$$
$$= T[\Phi_{xx}(1+\Phi_y^2)-2\Phi_x\,\Phi_y\,\Phi_{xy}+\Phi_{yy}(1+\Phi_x^2)](1+\Phi_x^2+\Phi_y^2)^{-3/2}, \quad z=\Phi,$$

where $\hat{\boldsymbol{n}}$ is the unit normal vector to the interface pointing into fluid 2. After linearization of this equation and using the expressions for initial state pressures in (10) and (11):

$$p_2-p_1+2\mu_1\,\mathrm{D}w_1-2\mu_2\,\mathrm{D}w_2 = -Tk^2\eta-(\rho_1-\rho_2)\,g\eta-\frac{B_0^2}{2\mu_0\,\delta}\eta, \quad z=0, \tag{30}$$

where T is the interfacial tension between fluids 1 and 2.

In order to determine the solution of (23), the particular solution, $\eta w_0(z)$, is expressed in the form $w_0(z)=X\mathrm{e}^{\alpha_+ z}+Y\mathrm{e}^{\alpha_- z}$, which already satisfies the boundary condition in (26), and the constants X and Y are

$$X = \frac{B_0^2k_x^2}{2\mu_0\mu_1\delta^3}\frac{\mathrm{i}(1+\mathrm{i})}{(\alpha_+^2-k^2)(\alpha_+^2-q_1^2)}\frac{(2+\mathrm{s}/\omega)}{(\gamma_++k)} \tag{31a}$$

and

$$Y = \frac{B_0^2k_x^2}{2\mu_0\mu_1\delta^3}\frac{-\mathrm{i}(1-\mathrm{i})}{(\alpha^2-k^2)(\alpha^2-q_1^2)}\frac{(2-s/\omega)}{(\gamma_-+k)}. \tag{31b}$$

Hence, the solution of (23) and (25) that also vanishes at infinity is conveniently written as

$$w_1(z) = \eta[M_1\,\mathrm{e}^{kz}+N_1\,\mathrm{e}^{q_1z}+w_0(z)], \quad z<0, \tag{32a}$$

$$w_2(z) = \eta[M_2\,\mathrm{e}^{-kz}+N_2\,\mathrm{e}^{-q_2z}], \quad z>0, \tag{32b}$$

where $q_1^2=k^2+\mathrm{i}s\rho_1/\mu_1$ and $q_2^2=k^2+\mathrm{i}s\rho_2/\mu_2$, such that the real parts of both q_1 and q_2 are positive and M and N are constants now to be determined.

Two of the constants, N_1 and N_2, are eliminated by applying the kinematic boundary condition in (27) and then the remaining two constants are determined using (28) and (29). Therefore, with the determinants defined as

$$D_1=\begin{vmatrix} Z_1 & k-q_2 \\ Z_2 & -\rho_2 \end{vmatrix}, \quad D_2=\begin{vmatrix} k-q_1 & Z_1 \\ \rho_1 & Z_2 \end{vmatrix}, \quad D_0=\begin{vmatrix} k-q_1 & k-q_2 \\ \rho_1 & -\rho_2 \end{vmatrix},$$

for Z_1 and Z_2 expressed as follows:

$$-[\mathrm{i}s(q_1+q_2)-w_0(0)\,q_1+w_0'(0)] = Z_1,$$

$$\{2k^2(\mu_1-\mu_2)+\mathrm{i}s(\rho_1-\rho_2)+\frac{\mu_1}{\mathrm{i}s}[w_0''(0)-q_1^2\,w_0(0)]\} = Z_2,$$

the perturbation velocities are established to be

$$w_1(z) = \eta\left\{\frac{D_1}{D_0}(\mathrm{e}^{kz}-\mathrm{e}^{q_1z})+[\mathrm{i}s-w_0(0)]\,\mathrm{e}^{q_1z}+w_0(z)\right\}, \quad z<0, \tag{33a}$$

$$w_2(z) = \eta\left\{\frac{D_2}{D_0}(\mathrm{e}^{-kz}-\mathrm{e}^{-q_2z})+\mathrm{i}s\,\mathrm{e}^{-q_2z}\right\}, \quad z>0. \tag{33b}$$

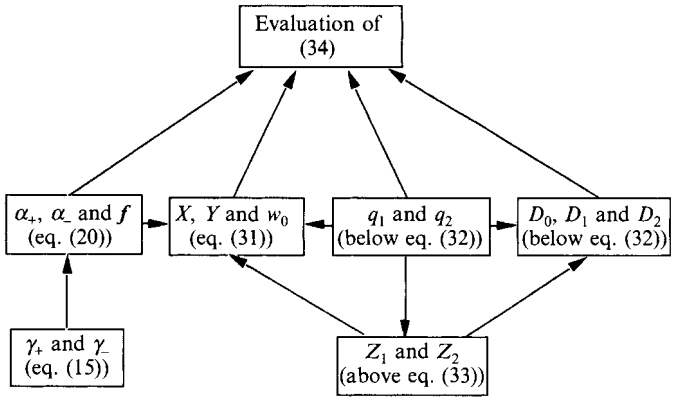

FIGURE 2. Computational scheme for (34).

The fluid velocities obtained here are inserted in (22) and (24) to compute the perturbation pressure. After some algebra, the difference in the perturbation pressure across the interface is thus determined as

$$p_1(z=0)-p_2(z=0)=\eta\left\{\left(\frac{\mu_1 q_1^2-\mu_2 q_2^2}{k^2}\right)\left[\frac{D_2}{D_0}(k-q_2)+\mathrm{i}sq_2\right]-\mathrm{i}\frac{(\boldsymbol{k}\cdot\boldsymbol{f})}{k^2}\right.$$
$$\left.+\frac{1}{k^2}\left[\frac{\mu_1 D_1(k^3-q_1^3)+\mu_2 D_2(k^3-q_2^3)}{D_0}+\mathrm{i}s(\mu_1 q_1^3+\mu_2 q_2^3)-\mu_1(w_0(0)\,q_1^3-w_0'''(0))\right]\right\}.$$

The final equation that establishes the criterion to determine stability or instability is obtained by substituting this pressure difference in (30) and eliminating η:

$$(\rho_1-\rho_2)g+Tk^2+\frac{B_0^2}{2\mu_0\delta}=\left(2(\mu_1-\mu_2)+\frac{\mu_1 q_1^2-\mu_2 q_2^2}{k^2}\right)\left[\frac{D_2}{D_0}(k-q_2)+\mathrm{i}sq_2\right]-\mathrm{i}\frac{(\boldsymbol{k}\cdot\boldsymbol{f})}{k^2}$$
$$+\frac{1}{k^2}\left[\frac{\mu_1 D_1(k^3-q_1^3)+\mu_2 D_2(k^3-q_2^3)}{D_0}+\mathrm{i}s(\mu_1 q_1^3+\mu_2 q_2^3)-\mu_1(w_0(0)\,q_1^3-w_0'''(0))\right], \quad (34)$$

where $\boldsymbol{f}$ is evaluated at $z=0$.

For given values of physical properties and operating conditions, and for specified $\boldsymbol{k}$, this equation is used to compute s. Because s is a complex quantity, (34) is actually two equations of real variables and constants, used to estimate both the real and imaginary parts of s. The technique used to determine s from (34) is similar to the bisection method, which here is applied in two dimensions (variables): the real part of s, $\mathrm{Re}(s)$, and the imaginary part of s, $\mathrm{Im}(s)$. The objective is the determination of $\mathrm{Re}(s)$ and $\mathrm{Im}(s)$ such that the difference between the left-hand and right-hand sides of the imaginary part of (34) (that difference henceforth called G) is zero, and similarly for the real part of (34) (henceforth H). A region of the $\mathrm{Re}(s)$, $\mathrm{Im}(s)$ plane is divided into small rectangles and G and H are evaluated at the corners of each rectangle. A rectangle where G changes sign between adjacent corners is traversed by the locus $G=0$, as is at least one adjacent rectangle. In this way $G=0$ is 'tracked'. H is evaluated on each corner of a traversed rectangle and tracking halted when a rectangle is encountered with a change of sign of H. That rectangle then contains a solution to (34) and is subdivided into smaller rectangles. The procedure is repeated until a solution is obtained with the necessary precision. As in many numerical techniques, the solution may not be unique. However, in the present work the $\mathrm{Re}(s)$, $\mathrm{Im}(s)$ plane has been explored over a wide range, much beyond what might be expected for the application

under consideration (electromagnetic casting) and only one solution found for positive values of $\mathrm{Re}(s)$. Figure 2 illustrates the order in which the required auxiliary variables are determined to solve (34).

If $\mathrm{Im}(s)$ is negative for a given $\boldsymbol{k}$, the system is unstable, and stable otherwise. Furthermore, $\mathrm{Im}(s)$ also provides the stated objective of this work, namely the growth or damping rate of the disturbance. $\mathrm{Re}(s)$ gives the angular frequency of the oscillations on the interface.

3. Application in EM casting of aluminium

In the context of EM casting of aluminium, in the preceding analysis the fluid 2 is air on top and fluid 1 is aluminium below. The physical properties for this system are listed in table 1.

In the absence of an EM field, the hydrodynamic system of a heavier fluid below a lighter one is unconditionally stable (Rayleigh–Taylor stability), that is perturbations will not grow. If the fluids are inviscid, because there is no mechanism for dissipation of mechanical energy, a perturbation imposed on the interface executes an undamped oscillation; for viscous fluids, however, the oscillations are damped. With an applied high-frequency magnetic field, Garnier & Moreau's (1983) analysis for inviscid fluids predicts stability, where the marginal state is characterized by undamped oscillations of the aluminium/air interface. For a magnetic field of amplitude 0.1 Tesla and 1 kHz frequency, the angular frequency, $\mathrm{Re}(s)$, predicted from their analysis is plotted as a function of dimensionless wavelength in a direction 45° from the X-axis (curve d in figure 3).

The present analysis differs from that of Garnier & Moreau in two respects: s was not neglected compared to ω (equation (15)) and viscosity was included. The addition of viscosity to Garnier & Moreau's analysis can be achieved within the scope of the present analysis merely by neglecting s in (15). The frequencies of the interface oscillations (curve a, figure 3) are identical to those of Garnier & Moreau. However, an imposed disturbance is damped as shown by the positive values of $\mathrm{Im}(s)$ (curve a, figure 4). Although a perturbation of short wavelength is rapidly damped when viscous effects are included, a perturbation of wavelength $(2\pi/k)$ greater than, say, 10δ persists for a long time. Consequently, this extension of the analysis of Garnier & Moreau suggests that viscosity may be an insufficient mechanism for avoiding oscillations of the melt surface in practical casters.

The algebra of the preceding section is sufficiently complicated that it is not obvious that the results reduce to those of Garnier & Moreau in the limit of zero viscosity (and negligible s). This was demonstrated numerically by repeating the calculations pertaining to figure 4 but with viscosities reduced to $\mu_1 = 1.2 \times 10^{-7}$ kg ms^{-1} (four orders of magnitude less than that of aluminium) and $\mu_2 = 30.8 \times 10^{-9}$ kg ms^{-1} (three orders of magnitude less than that of air); s was neglected compared to ω. The computed results appear in table 2 and demonstrate the approach to Garnier & Moreau's result ($\mathrm{Im}(s)$ zero) under these circumstances.

The effect of neglecting s in (15) is seen when s is included in the calculations, while the viscosity is ignored, and computed results are compared to those from Garnier & Moreau (1983). The $\mathrm{Re}(s)$ (curve b, figure 3) is identical to that of Garnier & Moreau but $\mathrm{Im}(s)$ is now negative (curve b, figure 4), implying instability. Therefore, the apparent conservation of mechanical energy implied by an undamped motion of the interface in Garnier & Moreau (1983) seems to arise due to neglect of s in calculations from the perturbed magnetic flux density. If s is included, the stable oscillations of

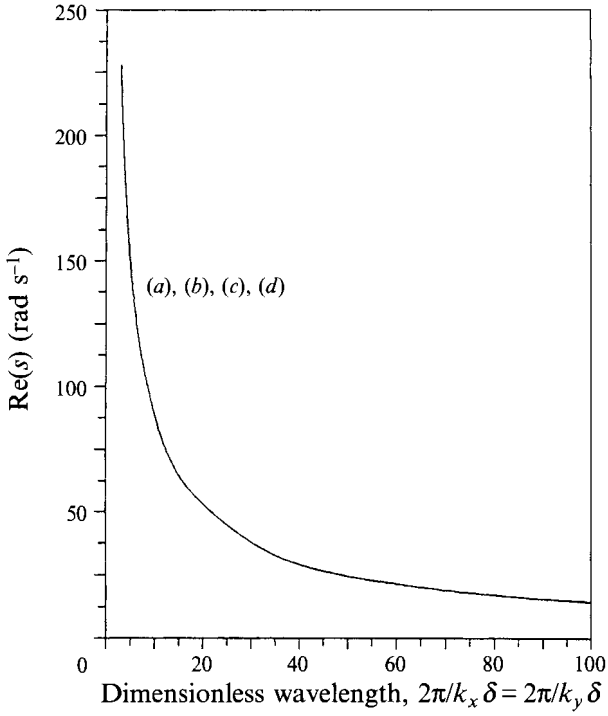

FIGURE 3. Re(s) *vs.* wavelength: (*a*) present analysis with s/ω neglected; (*b*) without viscosity, but s/ω not neglected; (*c*) present analysis with s/ω not neglected; (*d*) analysis of Garnier & Moreau. $B_0 = 0.1$ T, $f = 1$ kHz.

Conductivity of aluminium, σ (mho m^{-1})	3.85×10^6
Density of aluminium, ρ_1 (kg m^{-3})	2300
Density of air, ρ_2 (kg m^{-3})	0.5
Viscosity of aluminium, μ_1 (kg ms^{-1})	1.2×10^{-3}
Viscosity of air, μ_2 (kg ms^{-1})	30.8×10^{-6}
Aluminium/air interfacial tension (N m^{-1})	0.868

TABLE 1. Physical properties of aluminium and air

Garnier & Moreau's analysis are augmented for most wavelengths. The maximum growth rate for the conditions of the calculations occurs at a wavelength of approximately 10δ. As in the analysis of the previous paragraph, long wavelengths should be little affected by the magnetic field.

Use of the full analysis of the present work (that is, s is included in (15) and fluids are viscous) results in curve (*c*) of figures 3 and 4. Again the frequencies of the interface oscillations are the same but differences in the stability (imaginary part of s) are evident in figure 4. The destabilizing effect of an alternating magnetic field is shown by the present analysis. This is in contrast to the stabilizing effect of a steady magnetic field on Rayleigh–Taylor instability (Chandrasekhar 1981).

Table 3 and the following paragraph are an attempted rationalization of the difference between the Garnier/Moreau analysis and the present investigation.

The perturbed body forces are seen to be different in the Garnier/Moreau analysis and ours. Referring to (15) and (20), γ_+ and γ_- and α_+ and α_- are pairs of complex

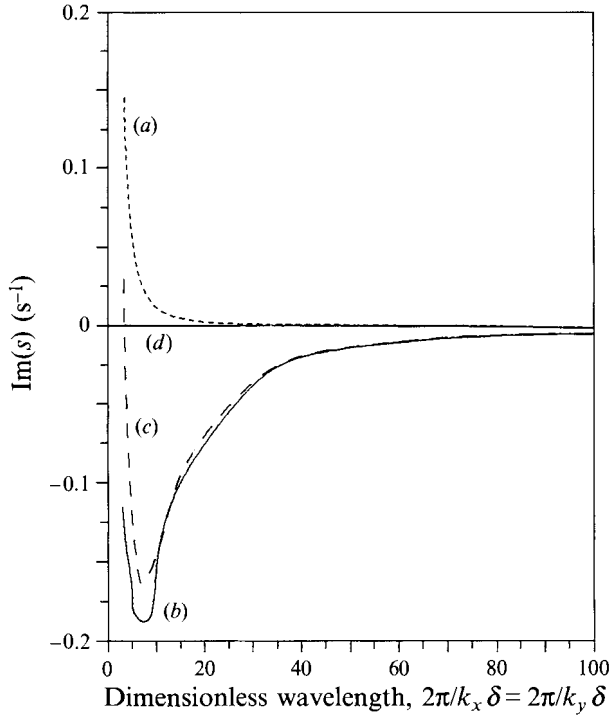

FIGURE 4. Im(s) *vs.* wavenumber: (*a*) present analysis with s/ω neglected; (*b*) without viscosity, but s/ω not neglected; (*c*) present analysis with s/ω not neglected; (*d*) analysis of Garnier & Moreau. $B_0 = 1$ T, $f = 1$ kHz.

Dimensionless wavelength	3	5	7	10	15	35
Im(s)	0.0004	0.0002	0.0001	0.0001	< 0.0001	< 0.0001

TABLE 2. Computed Im(s) for low viscosities ($\mu_1 = 1.2 \times 10^{-7}$ kg ms^{-1} and $\mu_2 = 30.8 \times 10^{-9}$ kg ms^{-1}) and s neglected, demonstrating convergence of results to those of Garnier & Moreau

Dimensionless wavelength	Perturbed forces	Garnier & Moreau	Present work
3	f_x	$0 + i42491067$	$84156 + i42490772$
	f_y	$0 + i126659952$	$0 + i126659952$
	f_z	$161324992 + i0$	$161326976 + i866779$
	$ik^2 f_z - D(\boldsymbol{k}\cdot\boldsymbol{f})$	$0 - i0.256 \times 10^{13}$	$-0.568 \times 10^{11} - i0.256 \times 10^{13}$
7	f_x	$0 + i37549444$	$92979 + i37549508$
	f_y	$0 + i54282836$	$0 + i54282836$
	f_z	$101608672 + i0$	$101612936 + i991672$
	$ik^2 f_z - D(\boldsymbol{k}\cdot\boldsymbol{f})$	$0 - i0.7655 \times 10^{12}$	$-0.108 \times 10^{11} - i0.7655 \times 10^{12}$

TABLE 3. Perturbed forces calculated from the analysis of Garnier & Moreau [1] and the present investigation. $\omega = 1$ kHz, $B_0 = 0.1$ T (conditions as in figure 4).

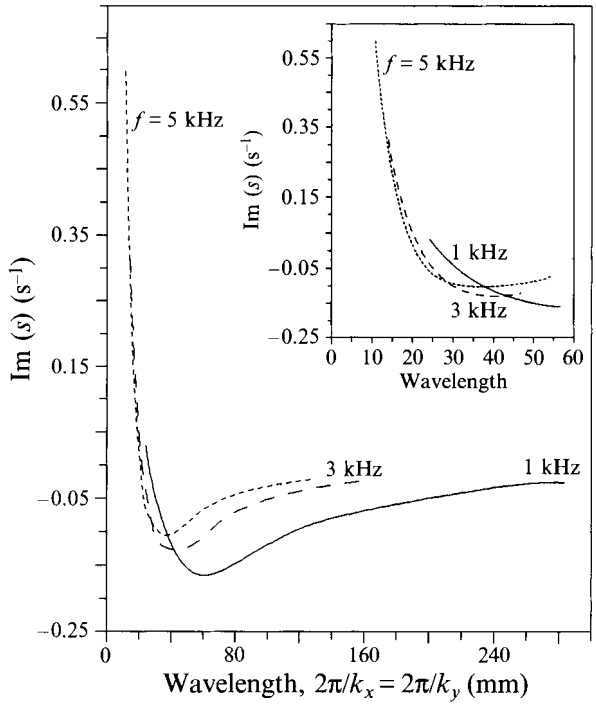

FIGURE 5. Effect of magnetic field frequency on growth rates of instability for perturbations 45° to the applied field. $B_0 = 0.1$ T.

conjugates in Garnier/Moreau; consequently the coefficients of the exponents in each of equations (16*a–c*) are also complex conjugates. As a result, components of f in Garnier/Moreau are either purely real or purely imaginary, as exemplified in table 3. In the present analysis, however, γ_+ and γ_- are not complex conjugates (nor are α_+ and α_-). Consequently the present analysis yields practically the same values for $\mathrm{Im}(f_x)$, $\mathrm{Im}(f_y)$ and $\mathrm{Re}(f_z)$ but now f_x and f_y have additionally a real part while f_z has an imaginary part. These additional parts lead to the growth or damping of the perturbations reported in the present work. Also appearing in table 3 is the 'driving force' for interface movement on the right-hand size of (23) and here again a significant difference is seen between the Garnier/Moreau analysis and that of the present paper in that the latter has a real part. However, inclusion of s in (15) has a negligible effect on $\mathrm{Im}(f_x)$, $\mathrm{Im}(f_y)$ and $\mathrm{Re}(f_z)$ (see table 3) and the angular frequency of the oscillations is therefore essentially identical in the present analysis and in Garnier/Moreau.

The following results are also for an applied field of $B_0 = 0.1$ T and wavenumbers inclined 45° on the X-axis, while the frequency of the applied field is varied. The results in this case are presented in figures 5 and 6 with wavenumbers not normalized by the skin depth, as the skin depth also depends on the frequency. At short wavelengths, the magnetic field of a higher frequency is more destabilizing, whereas beyond a wavelength of approximately 40 mm, a low-frequency magnetic field causes a greater instability, as shown in figure 5. The frequency range of the applied field of interest in EM casting of aluminium (2–5 kHz) does not have a significant effect on the oscillating frequency of the perturbed interface, as indicated by curves in figure 6 that correspond to frequencies in figure 5.

The strength of the magnetic field density required in EM casting of aluminium is on the order of 0.1 T. Figure 7 illustrates the effect of a magnetic field on the stability of

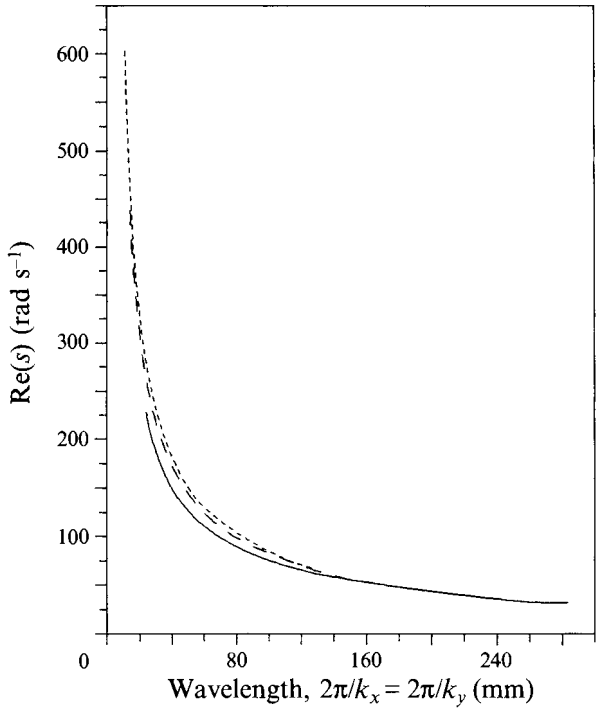

FIGURE 6. Effect of magnetic field frequency on oscillations at the interface for perturbations 45° to the applied field. Curves correspond to those in figure 5.

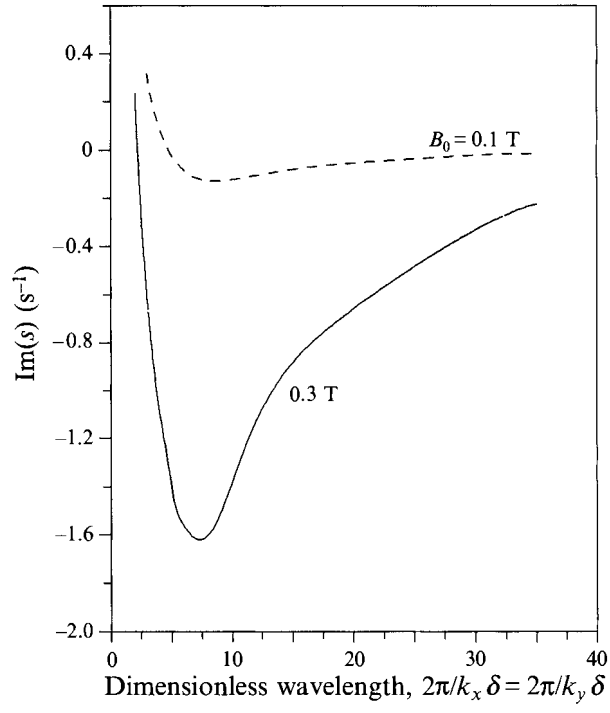

FIGURE 7. Effect of magnetic field strength on instability, Im(s) *vs.* wavelength. $f = 3$ kHz.

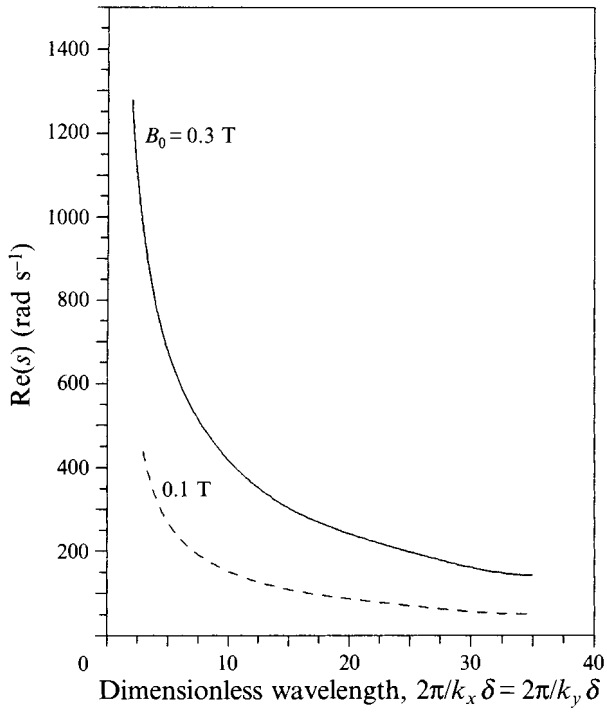

FIGURE 8. Effect of magnetic field strength on instability, Re(s) *vs.* wavelength. $f = 3$ kHz.

the system under investigation. Increased strength of the magnetic field is shown to cause a greater instability; only the short-wavelength perturbations are stable in the range of field strength examined here. (The wavelengths longer than 45δ behave the same way as in figure 4 and are included neither in figure 7 nor in the ones later.) Also, in this case, from figure 8, it is clear that a magnetic field of a greater strength leads to more rapid oscillations of the interface.

The effect of magnetic field strength is also examined for the wavenumbers in the direction of the magnetic field, the X-direction. As demonstrated in figure 9, when no magnetic field is applied to the system, it is always stable, which is a well-known result from the Rayleigh–Taylor analysis. Up to a field strength of approximately 0.025 T, the interface is stable. However, an application of an alternating magnetic field of increasing strength again causes a greater instability. In comparison to results in figure 7, for the same B_0 and similar wavenumbers, the growth rates, Im (s), are much higher for wavenumbers in the X-direction than those inclined 45° to it. The frequency of interface oscillation in figure 10, however, is similar to that in figure 8.

The disturbance with wavenumbers perpendicular to the applied magnetic field, that is the ones in the Y-direction, are unaffected by the field and hence are always stable. This fact is clear from (34) in which, for $k_x = 0$, the two terms $B_0^2/2\mu_0\delta$ and $-\mathrm{i}(\boldsymbol{k}\cdot\boldsymbol{f})/k^2$ cancel each other and w_0 is zero. Therefore, (34) becomes independent of the magnetic field, just as it would be if no field were applied. The results in that case exactly corresponds to those in figures 9 and 10 for $B_0 = 0$. Thus, the system is more stable to the wavenumbers away from the direction of the applied alternating field.

The value of the interfacial tension used in the calculations is for an aluminium/air interface. But it is known that the aluminium surface gets oxidized during the casting

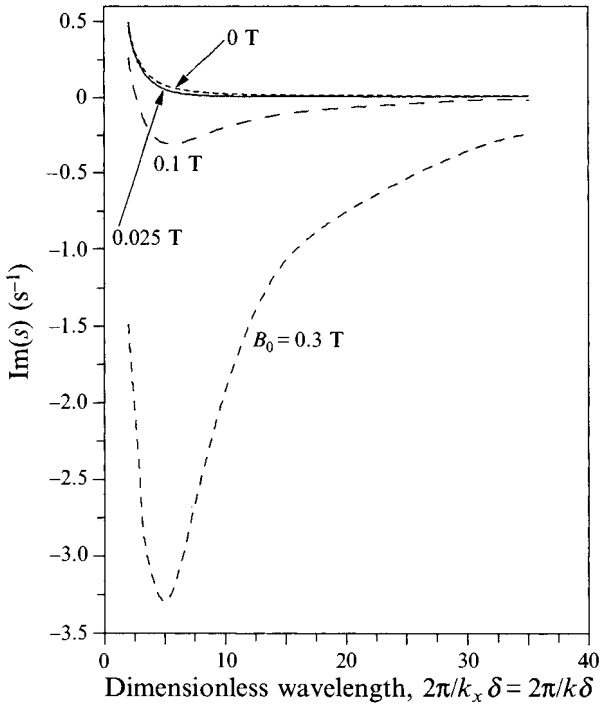

FIGURE 9. Growth rates for perturbation wavenumbers parallel to the applied field. $f = 3$ kHz.

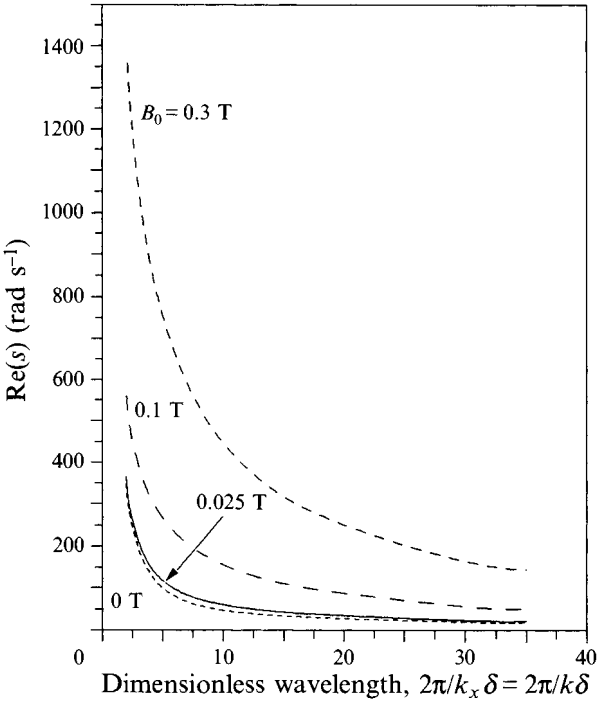

FIGURE 10. Oscillation frequency of the interface for perturbation wavenumbers parallel to the applied field. $f = 3$ kHz.

$\frac{2\pi}{k_x\delta} = \frac{2\pi}{k_y\delta}$	$T = 2.0$ N m^{-1}		$T = 0.868$ N m^{-1}		$T = 0$ N m^{-1}	
	Re(s) (rad s^{-1})	Im(s) (s^{-1})	Re(s) (rad s^{-1})	Im(s) (s^{-1})	Re(s) (rad s^{-1})	Im(s) (s^{-1})
2	1432.4	0.2417	1276.7	0.2317	1143.1	0.2212
4	815.66	−1.0699	782.7	−1.0727	756.4	−1.0751
15	304.7	−0.886	303.1	−0.8861	301.8	−0.8862

TABLE 4. Effect of interfacial tension. $B_0 = 0.3$ T, $f = 3$ kHz

operation and consequently there is uncertainty in the value of the interfacial tension. However, it is shown below that the interfacial tension has an insignificant effect on the instability.

At large wavelengths, the interfacial tension is not expected to have a notable effect. But even for the short wavelengths, the growth rate of the instability and the frequency of the interface oscillations are not significantly different when the stabilizing effect of the interfacial tension is ignored (table 4).

Experimental evidence from the work of Hull & Rote (1990) suggests that an alternating magnetic field delays the onset of Kelvin–Helmholtz instability on a horizontal surface of liquid metal. These workers report that, for field strengths of 10^{-3} to 10^{-2} T, the system in the presence of the field is able to tolerate larger gas velocities over the surface before instability occurs. In the present work we are not concerned with Kelvin–Helmholtz instability, and the critical field strength where instability occurs is higher (approximately 0.05 T) than those examined by Hull & Rote.

4. Conclusions

Not ignoring s in comparison to ω while determining the perturbed field radically alters the conclusions in Garnier & Moreau (1983); a stable system in that analysis is actually shown to be unstable. Because a similar hydrodynamic problem without the magnetic field constitutes a stable system, the presence of an alternating magnetic field is identified as the cause of instability.

Although viscosity of the fluids reduces the growth rates of the instability, the impact of viscosity is small under the conditions pertaining to EM casting. The disturbances of a short-to-intermediate wavelength grow most rapidly, and hence are likely to cause fluctuations on the interface. Furthermore, the long-wavelength perturbations ($> 40\delta$), with or without viscous effect, have a small growth rate. Hence, for all practical purpose, oscillations of corresponding frequency may be assumed to exist over the time period during which the metal solidifies. It is thus concluded that the striations on the cast ingot may be result of this instability and oscillations on the liquid metal surface.

The frequency of oscillations at the interface has been observed to be on the order of 10 rad s^{-1} (McHale & Melcher 1982). This frequency corresponds to the perturbations of wavelength more than 30δ, where a low frequency of the applied field causes a greater instability. Thus, EM casting of aluminium at a maximum admissible frequency may be better if electromagnetically induced surface oscillations are to be avoided.

As the origin of the instability is in the application of an alternating magnetic field, the casting operation should be carried out at a low strength of the field. That implies that the depth of liquid metal head supported by this field should be as small as possible.

The perturbations along the direction of the magnetic field are the most unstable, while those perpendicular to it are always stable. That demands additional care in avoiding disturbances parallel to the applied field.

The stability analysis presented in this paper cannot be regarded as a complete one for EM casting. The horizontal striations observed on the cast surface of an aluminium ingot are usually separated by a few millimetres and the casting speed is approximately 1 mm s^{-1}. That suggests that the striations would be caused by interface oscillations of frequency on the order of 1 Hz or less. However, in the results presented here, most frequencies are much higher. One possible explanation is that a broad range of frequencies is seen to be unstable and there may be beat frequencies between instabilities of closely spaced frequency that result in the observed surface imperfections.

This research was supported by the Bureau of Mines, US Department of Interior through the Generic Center for Pyrometallurgy, University of Missouri, Rolla, grant no. MU-USDI-G1135229-0642. The authors are grateful for additional support from Reynolds Metals Co.

REFERENCES

CHANDRASEKHAR, S. 1981 *Hydrodynamic and Hydromagnetic Stability*, pp. 428–512. Dover.

FAUTRELLE, Y. 1991 Free surface electromagnetic instabilities in liquid metals. In *Magneto-hydrodynamics in Process Metallurgy* (ed. J. Szekely, J. W. Evans, K. Blazek & N. El-Kaddah), pp. 63–68. The Minerals, Metals & Materials Society.

GALPIN, J. M., GILLON, P., GELFERT, Y. & FAUTRELLE, Y. 1990 Effects of a low frequency alternating magnetic field on a liquid metal. *ISIJ Proc. Sixth Intl Iron and Steel Congress, Nagoya*, pp. 362–369.

GARNIER, M. & MOREAU R. 1983 Effect of finite conductivity on the inviscid stability of an interface submitted to a high frequency magnetic field. *J. Fluid Mech.* **127**, 365–377.

Gupta, D. 1993 Electromagnetic processing: applications in ceramic composites and electromagnetic casting. PhD dissertation, University of California, Berkeley.

HULL, J. R. & ROTE, D. M. 1990 Stabilization of a molten-metal/coolant-gas interface by electromagnetic fields. *Phys. Fluids* A **2**, 443–446.

HULL, J. R., WIENCEK, T. & ROTE, D. M. 1989 Magnetohydrodynamic stability in the electromagnetic levitation of horizontal molten metal sheets. *Phys. Fluids* A **1**, 1069–1077.

MCHALE, E. J. & MELCHER, J. R. 1982 Instability of a planar liquid layer in an alternating magnetic field. *J. Fluid Mech.* **114**, 27–40.

RIVAT, P., ETAY, J. & GARNIER, M. 1991 Stabilization of a surface wave by a magnetic field. *Eur. J. Mech.* B/*Fluids* **10**, 537–551.

SNEYD, A. A. 1992 Interfacial instabilities in aluminium reduction cells. *J. Fluid Mech.* **236**, 111–126.

TAKEUCHI, S., ETAY, J. & GARNIER, M. 1989 Stability analysis of free surface of liquid metals levitated by electromagnetic force. *ISIJ Intl*, **29**, 1006–1015.

WINSTEAD, C. H. & HOBURG, J. F. 1991 Bulk-coupled electromechanical and electrothermal instability mechanisms in magnetically confined liquid metals. In *Magnetohydrodynamics in Process Metallurgy* (ed. J. Szekely, J. W. Evans, K. Blazek & N. El-Kaddah), pp. 45–53. The Minerals, Metals & Materials Society.

ZIMIN, V. D. & KOLPAKOV, N. YU. 1990 Magnetohydrodynamic flows and instability in the boundary of separation between the liquid metal and an electrolyte in aluminium reduction cells, **26**, 345–353.